

A SyR and IPM machine design methodology assisted by optimization algorithms

Original

A SyR and IPM machine design methodology assisted by optimization algorithms / F., Cupertino; Pellegrino, GIAN - MARIO LUIGI; Armando, Eric Giacomo; C., Gerada. - (2012), pp. 1-6. (Intervento presentato al convegno 2012 IEEE Energy Conversion Congress and Exposition (ECCE) tenutosi a Raleigh, USA nel 15-20 settembre 2012) [10.1109/ECCE.2012.6342478].

Availability:

This version is available at: 11583/2503167 since:

Publisher:

IEEE

Published

DOI:10.1109/ECCE.2012.6342478

Terms of use:

This article is made available under terms and conditions as specified in the corresponding bibliographic description in the repository

Publisher copyright

(Article begins on next page)

A SyR and IPM machine design methodology assisted by optimization algorithms

F. Cupertino
Politecnico di Bari - DEE
Bari, Italy
cupertino@poliba.it

G.M. Pellegrino, E. Armando
Politecnico di Torino - DENERG
Torino, Italy
gianmario.pellegrino@polito.it

C. Gerada
University of Nottingham
Nottingham, UK
chris.gerada@nottingham.ac.uk

Abstract— The design optimization of synchronous reluctance (SyR) machine and its extension to internal permanent magnet (IPM) motors for wide speed ranges is considered in this paper by means of a Finite Element Analysis-based multi-objective genetic algorithm (MOGA). The paper is focused on the rotor design, that is controversial key aspect of the design of high saliency SyR and IPM machines, due to the difficult modeling dominated by magnetic saturation. A three step procedure is presented, to obtain a starting SyR design with the optimal torque versus torque ripple compromise and then properly include PMs into the SyR geometry, given the desired constant power speed range of the final IPM machine. The designed rotors have been extensively analyzed by computer simulations and two SyR prototypes have been realized to demonstrate the feasibility of the design procedure.

I. INTRODUCTION

Synchronous reluctance motors are a viable alternative to induction motors because they allow a better torque to weight ratio. The power factor and the constant power speed range (CPSR) can be improved thanks to the insertion of permanent magnets in rotor layers. The obtained machine is referred to as a Permanent Magnet-assisted SyR motor or, simply, an Interior Permanent Magnet (IPM) synchronous motor [1,2]. One key-issue in the design of such machines is to define the rotor geometry, that presents many degrees of freedom (number and shape of the layers, PM grade and placement). Linear magnetic models are way too optimistic for such kind of motors, therefore analytical [3] and lumped parameter models [4] are always associated to Finite Element Analysis (FEA), in the literature, to account for magnetic saturation effects. Hybrid approaches such as frozen permeability have been also proposed [5]. Another fundamental aspect is the minimization of the torque ripple that can be very high in case of poor design choices and it is difficult to be modeled by simple formulas [6]. Optimization algorithms based on FEA evaluation of the motor performance have been proposed, but they suffer from being time-consuming [7], and they have often been applied to rotors with simple geometries, such as single layer rotors [8, 9], for having a limited number of degrees of freedom and then keep the computational time under control.

A comprehensive design approach based on FEA

optimization, like the one proposed in [10] for surface mounted PM motors is still under investigation for IPM motors because of their complicate rotor geometry, that involves a higher number of parameters. It is important to underline that the current phase angle giving the maximum torque is unknown a priori, and the flux weakening capability of the motor and then the CPSR are difficult to be evaluated quickly.

In [11], the basic ideas for evaluating different performance goals such as maximum torque per Ampere, torque ripple, CPSR and rotor losses with a very limited number of FEA runs have been proposed and tested, for a three-layer IPM rotor geometry.

This paper introduces a simpler procedure for the optimal design of multi-layer, IPM rotor machines, based on a two stage approach: first a SyR motor is designed and optimized for maximum torque and minimum torque ripple, and then the rotor layers are filled with plastic PM material, and the PM grade is calibrated, in post processing, for obtaining the required power versus speed characteristic.

The aim of the paper is to contribute to the definition of a standard design methodology, applicable also by non-specialist designers. The methodology utilizes multi-objective optimization algorithms to select rotor geometry but, with respect to previous literature, both the definition of the optimization problem and the interpretation of the results have been greatly simplified.

II. MULTI-OBJECTIVE GENETIC OPTIMIZATION (MOGA)

The design of an electric motor is a multi-objective problem, that is the quest for the optimal compromise between many conflicting goals. Multi-objective optimization algorithms search for a set of possible solutions according to the Pareto dominance criterion. Once the Pareto front is obtained the designer can select the preferred compromise solution, among the ones in the front, with a clear view of how each objective is penalized by the improvement of the other ones. Thus the human decision comes after the automatic solution and not before, that is what normally happens with single-objective optimization. It is very important that the functional evaluation, meaning the evaluation of all the goal functions for each tentative

solution, is computationally fast in order to permit a high number of iterations in a reasonable time. Computation time is, up to date, the actual bottleneck of FEA-based optimization. Even if, in theory, it could be possible to solve multi-objective optimization problems with a relatively high number of conflicting goals, there are two problems that arise with the increase of the optimization complexity. First, an accurate estimate of the Pareto front needs an adequate number of Pareto-optimal solutions and this number grows exponentially with the size of the objective vectors. As a consequence the number of possible solutions to be analyzed and the computation time are increased. The second problem regards the interpretation of the results. While a Pareto front for a two objectives problem is a simple curve into a plane, when the objectives are more than three there is no geometrical representation of the front and the choice of the solution that realizes the best compromise among the design objectives becomes a non-trivial task. The advantage of adopting an automated design procedure partially vanishes in case this requires the intervention of a machine specialist, to give a correct interpretation of the results. In this paper we propose a design procedure that adopts optimization algorithms only to solve relatively simple, two-objective problems in several optimization steps. The human expertise is only needed for design choices regarding practical aspects, such as the feasibility of the laminations cut, and a non-IPM specific motor design expertise is sufficient for obtaining a correctly optimized design..

III. PROBLEM STATEMENT

The stator geometry is then completely defined. Although it could be possible to extend the design optimization also to the stator, the design of the rotor (flux barriers and permanent magnets) is only considered here, being the most controversial and less standardized point in the design of such kind of machines. The rated current i_0 is calculated according to the accepted thermal load, expressed in stator Joule losses. The number of turns is chosen preliminarily, to be corrected at the final stage of the design, for adapting the voltage level of the selected machine to the willed ratings. The acceptable losses depend on the motor size and type of cooling. The rotor geometry is defined in figure 1 for a 2 pole-pairs, 3 layers IPM motor.

For the sake of a simple modelling, bonded magnets are assumed, filling the rotor layers completely: this way the PM flux linkage is dominated by the single parameter, B_r , that is the remanence of the PM. With filled, multiple layers, the values of B_r , for all practical applications are quite low, between 0.2 T and 0.45 T, depending on the number of layers and the current loading. Such remanences match well with plastic Nd materials, and also with low cost, hard ferrites. Still, the modelling approach is of general validity, including the case of sintered rare earth materials: once the optimal machine is obtained, the low remanence magnets filling the layers can be substituted with smaller, equivalent quantities of sintered magnets, giving the same performance.

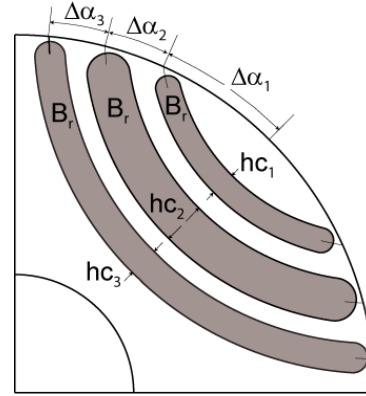


Fig. 1. Rotor geometry with 3 layers: the $\Delta\alpha_j$ angles define the layer angular positions, hc_j are the layer heights and B_r defines the PM grade

Let $n_{lay} = 3$ be the number of rotor layers. The set of parameters that define the IPM design consists of:

- three $\Delta\alpha_j$ angles, that define the layer positions at the airgap;
- three layer heights hc_j ;
- the remanence B_r ;
- the current phase angle γ .

That is a 8-dimensional space of the inputs, for the 3 layer example. B_r will be chosen in post processing, as explained in the following. Of course the number of parameters and the computational time would increase with more layers. Machines with four or five layers would give a better performance (less torque ripple, less PM quantity, lower back-EMF at given torque), but at the expense of a longer computational time and a more complicated manufacturing. The number of layers is considered here as a preliminary choice of the designer. An example with a 3-layer rotor is shown in the paper.

IV. DESIGN PROCEDURE

The proposed design procedure can be divided into three consecutive steps, referred to as:

1. Global Search MOGA (GS-MOGA) of a SyR machine
2. Local Search MOGA refinement (LS-MOGA)
3. Off-line definition of the PM remanence B_r

At first the PM remanence is set to zero and the rotor geometry is optimized (i.e. the $\Delta\alpha_j$ angles and the layer heights hc_j are defined). A two objectives GA run that maximizes the torque and minimizes the torque ripple is adopted. A set of geometrical constraints is imposed to ensure that the output geometry is mechanically feasible and has the adequate mechanical robustness. This first step is the global search (GS-MOGA). At the end of GS-MOGA, one solution machine is manually selected from the Pareto front (referred to as GS-solution) on the basis of both its performances (torque, torque ripple), feasibility, and

mechanical robustness (regularly spaced layers tend to be preferred).

The second optimization step consists of a refinement of the machine output by GS-MOGA. A second two objectives GA run is performed but this time the constraints are close to the parameters of the GS-solution: a plus or minus 15% change is allowed for each single parameter. This second optimization step is referred to as local search (LS-MOGA). The two steps procedure allows a good precision in finding a good approximation of the optimal solution with a reasonably low computational time (e.g. 10 hours for a three layer geometry).

As an alternative, a computationally intensive single MOGA run with a higher number of iterations could be adopted. Furthermore the use of hybrid algorithms based on both global and local search algorithms were investigated but revealed to be more expensive in terms of computational cost.

The third and final design step consists of the introduction of permanent magnets. Keeping the layer geometry of the LS-solution, the remanence of the permanent magnets is chosen according to the flux weakening range required by the application.

V. SIMULATION RESULTS

The described design procedure has been implemented using standard software tools such as MATLAB and the freeware FEMM [12]. The example design refers to an existing IPM motor for home appliances, rated 1400 W at 7200 rpm.

Both GS- and LS-MOGA stages refer to a population of 60 solutions and 50 iterations. Each MOGA run takes approximately 5 hours on a laptop with a 2.7 GHz Intel i7 CPU. To the aim of optimizing the overload capabilities, the stator current was set to $2 \cdot i_0$ during the MOGA runs, i_0 being the motor current rating for continuous operation. Figure 2a compares the rotor designs obtained using GS-MOGA and LS-MOGA. It is possible to notice that the intermediate layer is the thickest one, while in most of related literature the layers thicknesses are progressive or all equal. Moreover, the local search run refines the layer thicknesses without changing the layer angular positions at the airgap. Figure 2b shows a detail of the Pareto front obtained with LS-MOGA, including the selected GS-solution. It evidences how the LS-MOGA slightly improves the torque but drastically reduces the torque ripple. This is confirmed also by figure 3, in which the torque waveforms at different current levels are shown. Figure 4 shows the torque ripple maps versus the i_d and i_q current components for GS-solution and LS-solution. The optimized design (LS) has a lower ripple at any current load and phase angle. It is worth to underline that the minimum torque ripple in the i_d - i_q plane closely follows the expected maximum torque per ampere (MTPA) trajectory of an IPM machine.

The final step of the design procedure consists in the inclusion of permanent magnets in the rotor.

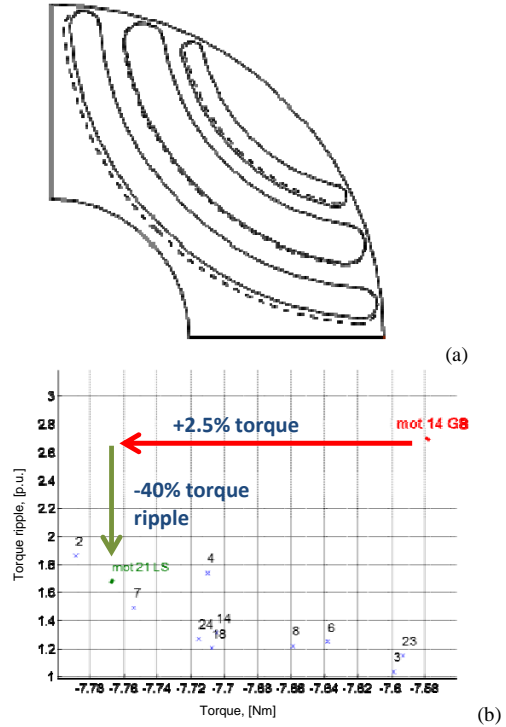


Fig. 2. (a) Rotor geometry obtained by the GS-MOGA (dashed line) and then refined by LS-MOGA (continuous line). (b) Detail of the Pareto fronts obtained with GS-MOGA (blue) and LS-MOGA (red) that evidences the selected solutions and the amount of performance improvement.

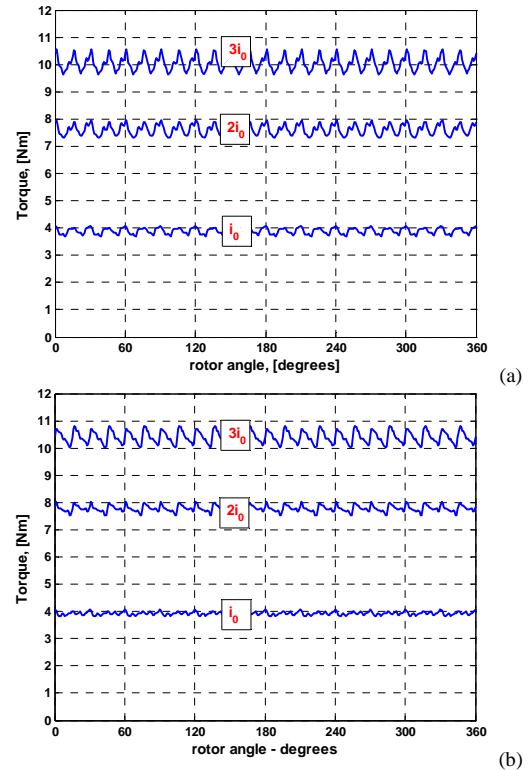


Fig. 3. Torque-position waveforms for GS-solution (a) and LS-solution (b) calculated with the respective MTPA current phase angles

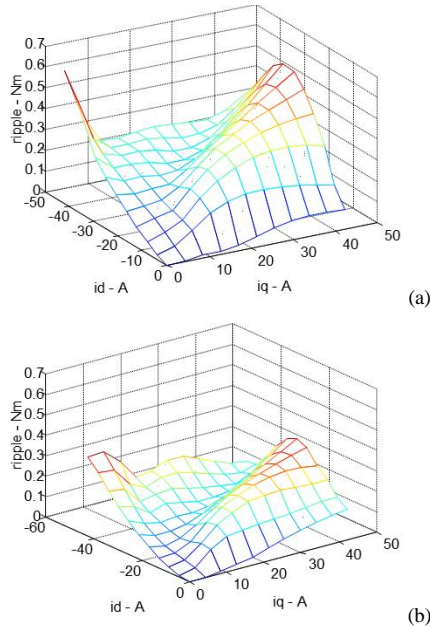


Fig. 4. Torque ripple maps over the $i_d - i_q$ plane for (a) the GS-solution and (b) the LS-solution.

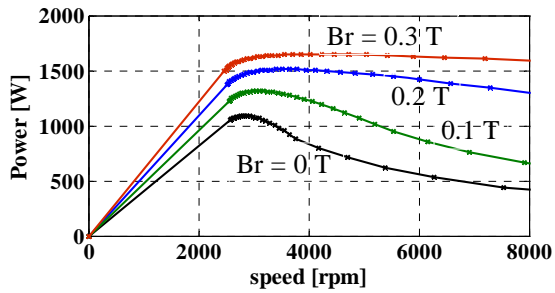


Fig. 5. Power-speed profiles of the LS-solution with different PM remanence values.

Figure 5 shows the power-speed profiles of the LS-solution with different magnet residual flux density. The latter has been increased until the desired constant power speed range was satisfied. This has been achieved with bonded magnets with $B_r=0.2$ T. As said, practical construction can be realized either with an injection of plastic bonded material, or with discrete blocks of low cost ferrite filling the space almost completely or also with smaller bricks of sintered neodymium magnets. Such a degree of freedom is a key advantage of the proposed design methodology considering the reduced availability and increasing cost of high power magnets.

VI. EXPERIMENTAL RESULTS

Two rotor prototypes have been realized to validate the first step of the proposed design procedure. Both of them are SyR motors and figure 6 reports a picture of their rotor laminations. The one in subfigure (a) is the LS-MOGA, designed after the second iteration of the optimization

process. The other prototype has been designed following the state of the art design criteria of [13], and will be set as the benchmark to evaluate the performances of the genetic-algorithm generated rotor. The torque ripple maps versus the i_d and i_q current components for both considered SyR motors have been measured using a dedicated test bench. A DC motor having very low torque ripple is coupled to the motor under test using a gearbox with reduction ratio equal to 50. The shaft torque is measured with an high precision torque meter. The rotor speed is kept constant and equal to 10 rpm by the DC motor. The motor under test is vector current controlled, using a dSPACE 1104 board. A Matlab script has been realized to set the current references automatically and measure the torque during one motor revolution. The torque-meter rating has suggested not to exceed the 20 A per 20 A current area. The test bench is shown in figure 7.

Figure 8 compares the average torque maps over the $i_d - i_q$ plane obtained for LS-MOGA motor (a) and for the benchmark motor (b) using both computer simulations and experiments. A similar comparison of the torque ripple maps over the $i_d - i_q$ plane is reported in figure 9. Simulation and experimental results are generally in good agreement. An appreciable difference occurs when i_d current is close to zero but this region is far from the MTPA characteristic of both machines. On average, the measured torque ripple of both the prototypes is slightly higher than the one obtained with simulations

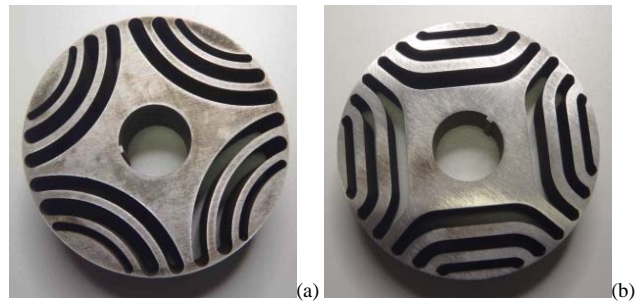


Fig. 6 – Rotor laminations: LS-MOGA rotor (a) and benchmark rotor (b).

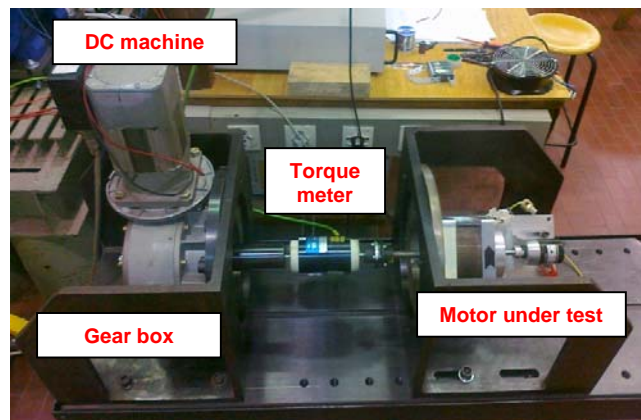


Fig. 6 – Test bench used to measure the torque ripple maps of the motor prototypes.

Even if the laminations have been realized using a high precision wire cut Electric Discharge Machining (EDM), it is reasonable that the increased torque ripple is justified by machining and assembling processes. Figure 10 the measured torque waveforms at different current levels are shown. As foreseen by FEA calculations, the benchmark rotor produce a higher average torque, also thank to a better utilization of rotor iron outside the smaller layer. On the other hand the LS-MOGA rotor guarantee a lower torque ripple, in particular at overload. We are currently considering alternative rotor geometries, suitable for automatic optimization but capable of a better exploitation of the rotor iron, comparable with the one of the benchmark machine.

VII. CONCLUSION

This paper has introduced an automatic design procedure to design SyR motors, and to obtain a PM-assisted or IPM machine from the automatically designed SyR one. The procedure is based on Finite Element Analysis and a multi-objective genetic algorithm (MOGA). A simple rotor geometry has been selected so to minimize the number of parameters used to define each potential solution and to speed up the optimization process. Experimental results demonstrate that, in spite of the simple geometry, the automatically designed machine has a torque versus current performance that is comparable to the one of more complicated designs, while giving a lower torque ripple.

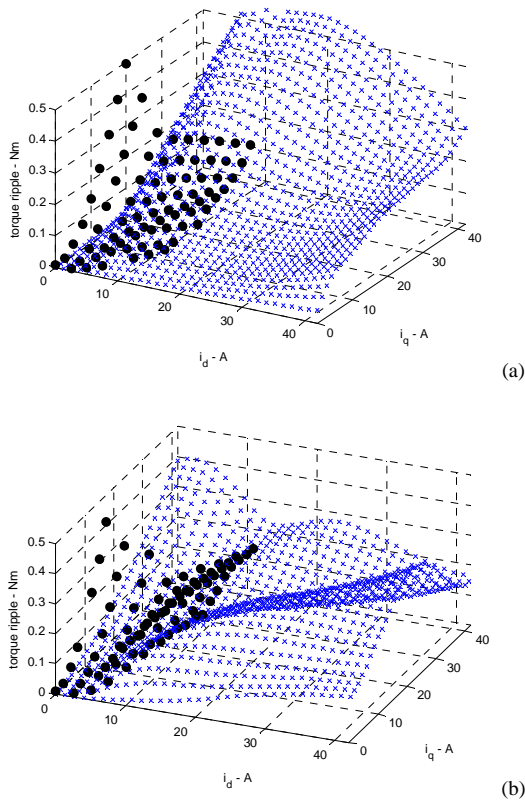


Fig. 7. Torque ripple maps over the $i_d - i_q$ plane for (a) the benchmark motor and (b) the LS-MOGA motor: comparison of FEM results (blue x) and experimental results (black dots).

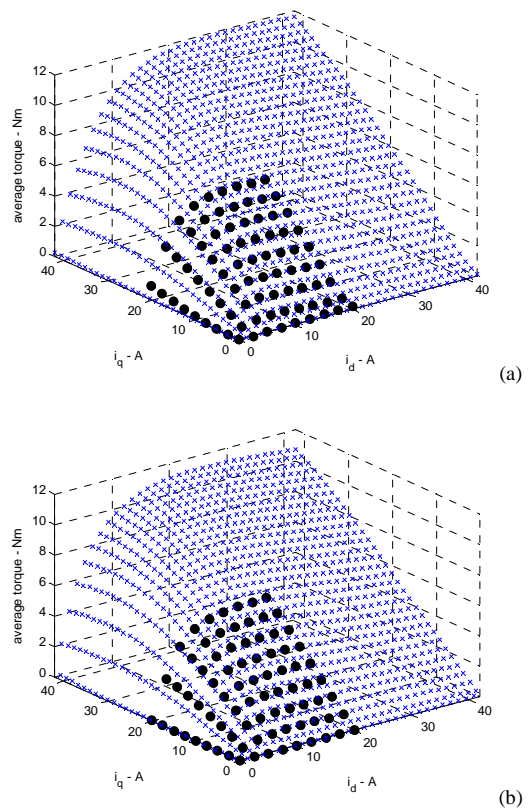


Fig. 8. Average torque maps over the $i_d - i_q$ plane for (a) the benchmark motor and (b) the LS-MOGA motor: comparison of FEM results (blue x) and experimental results (black dots).

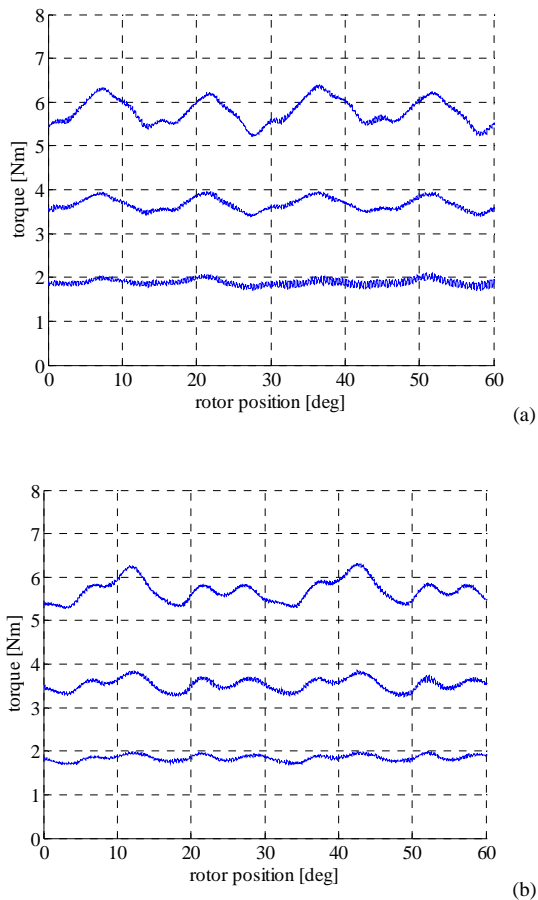


Fig. 10. Experiments: torque-position waveforms for (a) the benchmark motor and (b) the LS-MOGA calculated with the respective MTPA current phase angles

REFERENCES

[1] R. Schiferl, T.A. Lipo, "Power capability of Salient pole P.M. synchronous motors in variable speed drive", Conf. Record. of IEEE- IAS annual meeting 1988, pp: 23-31.

[2] W. Soong and T. J. E. Miller, "Field weakening performance of brushless synchronous AC motor drives," Proc. IEE—Elect. Power Appl., vol. 141, no. 6, pp. 331–340, Nov. 1994.

[3] A. Fratta, A. Vagati, F. Villata, "Design criteria of an IPM machine suitable for field-weakening operation", International Conference on Electrical Machines, ICEM90, Boston 1990, U.S.A., pp: 1059-1065.

[4] Lovelace, E.C.; Jahns, T.M.; Lang, J.H., "Impact of saturation and inverter cost on interior PM synchronous machine drive optimization," Industry Applications, IEEE Transactions on , vol.36, no.3, pp.723-729, May/June 2000.

[5] Tangudu, J.K.; Jahns, T.M.; El-Refaei, A.M.; Zhu, Z.Q.; , "Segregation of torque components in fractional-slot concentrated-winding interior PM machines using frozen permeability," Energy Conversion Congress and Exposition, 2009. ECCE 2009. IEEE , vol., no., pp.3814-3821, 20-24 Sept. 2009

[6] Jahns, T.M.; Soong, W.L., "Torque Ripple Reduction in Interior Permanent Magnet Synchronous Machines Using the Principle of Mutual Harmonics Exclusion," Industry Applications Conference, 2007. 42nd IAS Annual Meeting. Conference Record of the 2007 IEEE , vol., no., pp.558-565, 23-27 Sept. 2007

[7] Wen Ouyang; Zarko, D.; Lipo, T.A., "Permanent Magnet Machine Design Practice and Optimization," Industry Applications Conference, 2006. 41st IAS Annual Meeting. Conference Record of the 2006 IEEE , vol.4, no., pp.1905-1911, 8-12 Oct. 2006

[8] Bianchi, N.; Canova, A.; , "FEM analysis and optimisation design of an IPM synchronous motor," Power Electronics, Machines and Drives, 2002. International Conference on (Conf. Publ. No. 487) , vol., no., pp. 49- 54, 4-7 June 2002

[9] Sizov, G.Y.; Ionel, D.M.; Demerdash, N.A.O.; , "Multi-objective optimization of PM AC machines using computationally efficient - FEA and differential evolution," Electric Machines & Drives Conference (IEMDC), 2011 IEEE International , vol., no., pp.1528-1533, 15-18 May 2011

[10] Bianchi, N.; Bolognani, S., "Design optimisation of electric motors by genetic algorithms," Electric Power Applications, IEE Proceedings - , vol.145, no.5, pp.475-483, Sep 1998.

[11] Pellegrino, G.; Cupertino, F.; , "FEA-based multi-objective optimization of IPM motor design including rotor losses," Energy Conversion Congress and Exposition (ECCE), 2010 IEEE , vol., no., pp.3659-3666, 12-16 Sept. 2010

[12] D.C. Meeker, Finite Elements Method Magnetics, Version 4.0.1 (03 Dec 2006 Build), <http://www.femm.info>.

[13] Vagati, A.; Pastorelli, M.; Francheschini, G.; Petrache, S.C.; , "Design of low-torque-ripple synchronous reluctance motors," Industry Applications, IEEE Transactions on , vol.34, no.4, pp.758-765, Jul/Aug 1998